

## Thermal Effects of Fluid on Nanometric Cutting of Silicon

Guokun Qu<sup>1</sup> and Yongbo Guo<sup>2</sup>

<sup>1</sup>*School of Basic Science, Harbin University of Commerce, Harbin, China*

<sup>2</sup>*School of Mechatronics Engineering, Harbin Institute of Technology, Harbin, China*

*E-mail: quguokun@126.com*

### Abstract

*To understand the effect of fluid on thermal behavior of material removing in nanoscale, molecular dynamics (MD) simulation method is performed to model the chip generation, heat distribution, phase transformation and the temperature dependence by considering the effects of fluid during nanometric cutting of mono-crystalline silicon. In this work, a fluid containing model was used by considering fluids like coolants and concentrating on its impact during machining. The simulation results show that the chip size is 8% larger in vacuum than in the fluid containing model at the same simulation stage. In both case, the heat distribution topology is unanimous and roughly presents a concentric shape, a steep temperature gradient is observed in tool and the highest temperature lies in chip, but the average temperature is decreased of 6% in the low temperature ranges and 15% in chips of the fluid containing model. Phase transformation mainly occurred in chip, shear zone and machined surface, the growth of phase transformation is retarded by a volume decrease of 9% in the fluid containing model. Some physical quantities are decreased with the increasing system temperature during machining and show thermal soft effect.*

**Keywords:** *Molecular dynamics, Nanometric cutting, Heat distribution, Phase transformation.*

### 1. Introduction

In the rapid development of modern technologies and manufacturing of nanoscale device, mono-crystalline silicon is a widely used material in micro-electro-mechanical systems (MEMS) and nano-electro-mechanical systems (NEMS). Understanding the basic action of how material removing in nanoscale is a critical issue of producing well-formed components. The material removing, actually, is the removing of surface atoms and subsurface atoms, at such a small governing length scale, traditional continuum representation of the problem is become questionable. Though computational simulation, atomic-scale material removing process can be observed and analyzed directly. The first-principle simulations, which implement the electronic degrees of freedom, provide the insight into the microscopic mechanisms involved in the active role of bonds, the computation time, however, is very costly [1]. In addition, the continuum finite element method (FEM) has been used, this continuum approach can simulate cutting process up to several tens of nanometres, but have many disadvantage because of the sample phenomenological constitutive models [2]. As a complement of this problem, the quasi-continuum (QC) method was applied to simulate nanometric cutting process. These continuum and QC approaches can not capture the cutting phenomena in atomic scale, such as phase transformation and grain boundary sliding. So a new approach for numerical modelling is necessary. Since 1990s, molecular dynamics (MD) has been used to study cutting mechanism in atomic scale. Some typical work has been done by many researchers [3-6].

The previous work provides significant insight into workpiece-tool interactions phenomena and mechanical aspects. Little research has been done in studying the influence of environmental conditions such as atmosphere or fluid, these environmental factors, however, have significant effect on the performance of system during nanometric cutting process and hard to measure by experiment. Up to now, in the published research work, Rentch et al simulated the effects of fluid on the surface generation in material removal process of copper [7]. Lin et al investigated the effect of atmosphere in ultra-micro cutting by modifying the potential of surface atoms of diamond tool and silicon workpiece [8]. Considering fluid into account represents a more completely thermal equilibrium and heat convection during machining. Since the basis of coolant is water, the main object of this study is the use of MD simulation to evaluate the effect of water on thermal behavior during material removing process. The chip formation, heat distribution and phase transformation during machining are investigated based on Tersoff potential and long-range Lennard-Jones (LJ) potential. Two molecular dynamics simulations, one with water adding into simulation cell and the other without water, were conducted to understand the thermal effect of water during nanometric cutting process. The simulation results are shown in 3D images and analyzed in detail.

## 2. Simulation Methodology

The MD model of nanometric cutting is shown in Figure 1, in which workpiece and tool are composed with mono-crystalline silicon and diamond, respectively. The atomic model has the size of  $48 \text{ nm} \times 27 \text{ nm} \times 5 \text{ nm}$ . The employed process model considered about 350,309 fully dynamic atoms. Both workpiece and tool are divided into fix atoms, thermostat atoms and Newton atoms, to represent a more reality machining model. The green and mauve colored 'L' shaped area of the outer surface of workpiece and tool represent the area of fixed atoms, next to the fix atoms is the area of thermostat atoms and the rest are Newton atoms zone. Periodic boundary condition is imposed in the Z direction. This means, that in reality the present study's workpiece and tool are not a cuboids and pyramid but a chain of overlapping cuboids and prism, respectively. The fix boundary atoms are fixed in positions to reduce the boundary effects and maintain proper symmetry of lattice. A reflection wall is used in the outer surface of water atoms to maintain the density and pressure of water unchanged. The motion of Newton and thermostat atoms obeys Newton's second law. The temperature of thermostat atoms is stabilized at 300K during machining. Newton layer atoms are marked as grids in order to ease tracking of lattice deformation. The top surface of workpiece is (100) plane and the X direction is in the [100] orientation. The cutting speed is set as 300 m/s for saving simulation time and the corresponding cutting depth is 1.5 nm. The initial velocity of silicon and carbon atoms were assigned based on Maxwell distribution, Velocity-Verlet algorithm was applied to the time integration method, and the integration time step size was set as 0.5 fs, the time interval was a relatively small value compared to the oscillation frequency between carbon and silicon. Details of the simulation parameters are summarized in Table 1.

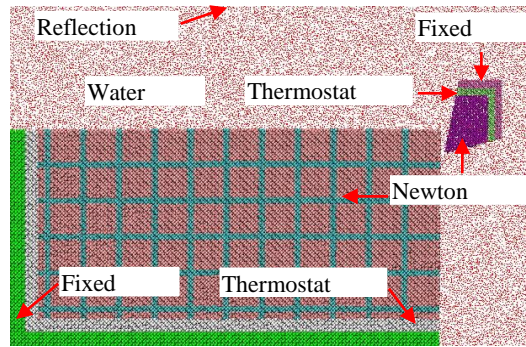


Figure 1. The Initial MD Simulation Model for Nanometric Cutting

Table 1. Simulation Parameters

Potential	Tersoff and LJ
Substrate material	Mono-crystalline silicon
Dimensions	48 nm × 27 nm × 5 nm
Number of atoms	350,309
Clearance angle $\alpha_r$	10°
Rake angle	8°
Cutting direction	[100] on (100) surface
Cutting depth	1.5 nm
Cutting speed	300 m/s
Initial temperature	300 K
MD Time step	0.5 fs

Initially, workpiece and tool were relaxed in a NPT assemble with the pressure controlled in 0.1 Mpa and the temperature fixed at 300 K for 30 ps, after adding the TIP3P water into system, sampling was carried out in a NVT assemble for 10 ns and the density of water was kept at 1.0 g/cm<sup>3</sup>. Distinct empirical potentials appropriate in simulation the C-C, Si-Si, Si-C and O-O bonding was employed, respectively. Tersoff potential is found to be suitable for describing the interactions between atoms with covalent bond [9-11]. In current simulation, the interactions between silicon atoms of the substrate and also between carbon atoms of tool were depicted by Tersoff potential. In all case, before leftwards movement, the tool was initially held at a distance (0.6 nm) larger than the cutoff distance for the Tersoff SiC potential ( $r_{cut}=0.3$  nm) in the right side of workpiece.

The Tersoff potential, as a function of coordinates, is given by:

$$E = \sum_i E_i = \frac{1}{2} \sum_{i \neq j} V_{ij},$$

$$V_{ij} = f_C(r_{ij}) [f_R(r_{ij}) + b_{ij} f_A(r_{ij})] \quad (1)$$

$$f_R(r_{ij}) = A \exp(-\lambda r_{ij}),$$

$$f_A(r_{ij}) = -B \exp(-\mu r_{ij}) \quad (2)$$

$$f_C(r_{ij}) = \begin{cases} 1, & r_{ij} < R \\ \frac{1}{2} + \frac{1}{2} \cos \left[ \pi \frac{r_{ij} - R}{S - R} \right], & R < r_{ij} < S \\ 0, & r_{ij} > S \end{cases} \quad (3)$$

$$b_{ij} = \left( 1 + \beta_i^n \xi_{ij}^n \right)^{-1/2n},$$

$$\xi_{ij} = \sum_{k \neq i, j} f_C(r_{ik}) \omega_{ik} g(\theta_{ijk}),$$

$$g(\theta_{ijk}) = 1 + \frac{c^2}{d^2} - \frac{c^2}{d^2 + (h - \cos \theta_{ijk})^2} \quad (4)$$

where  $E_i$  is the site energy,  $V_{ij}$  is the bond energy about all the atomic bonds,  $i, j, k$  label the atoms of the system,  $r_{ij}$  is the length of the  $ij$  bond,  $b_{ij}$  is the bond order term,  $\theta_{ij}$  is the bond angle between the bonds  $ij$  and  $ik$ ,  $f_R$  represents a repulsive pair potential,  $f_A$  represents attractive pair potential,  $f_C$  merely represents a smooth cutoff function to limit the range of the potential, and  $\xi_{ij}$  counts the number of other bonds to atom  $i$  besides the  $ij$  bond.

The present research is concentrated on the thermal aspects during machining, neglecting chemical effects, surfaces were assumed to be passivated, and both the physisorption and chemisorption of surfaces were not considered here. The long-range Lennard-Jones (LJ) potential,  $U(r)$ , is performed to describe the O-O interactions of water molecular as follows [12]:

$$U_{LJ}(r) = 4\varepsilon \left[ \left( \frac{\sigma}{r} \right)^{12} - \left( \frac{\sigma}{r} \right)^6 \right] \quad (5)$$

where  $\sigma$  ( $\sigma_{OO}=3.1507 \text{ \AA}$ ) is the equilibrium distance with minimum energy and  $\varepsilon$  ( $\varepsilon_{OO}=0.102 \text{ kJ mol}^{-1}$ ) is the potential depth determining the energy scale. The particle-particle particle-mesh (PPPM) algorithm has been used to account for the electrostatic interactions, while the LJ interactions were truncated at  $10 \text{ \AA}$ .

The conversion between the kinetic energy and temperature of each atom can be computed at each time step, as the follows equation:

$$\sum \frac{1}{2} m v^2 = \frac{3}{2} N k_B T \quad (6)$$

where  $N$  is the number of atoms,  $v_i$  represents the instantaneous velocity,  $k_B$  is the Boltzmann constant equal to  $1.38 \times 10^{-23} \text{ J/K}$  and  $T$  represents the temperature of atoms. However, the kinetic energy of per atom could not be transformed into temperature immediately, the velocity of atoms should be averaged and reassigned to each atom every  $N$  steps. For the sake of comparing the simulation result with macroscopic thermo-mechanism properties suitable data average algorithm should be taken. The contribution of tool movement in the cutting direction should not be included in computing kinetic energy. More rigorously, the contribution from angular motion of atoms should be taken into consideration. The simulation results revealed that an average over about 2000 time steps led to significantly stable mean properties, but still provide a certain time resolution

to study some dynamics of the cutting process. The velocity of thermostat atoms is rescaled when the temperature departs more than 10 K of the specified temperature. The various temperature zones are coded by different colors to distinguish heat distribution in workpiece and diamond tool during cutting process.

### 3. Results and Discussion

#### 3.1 Material Removing Characteristics

Figure 2 shows a snapshot of material removal process with water after 35 ps and the corresponding cutting distance is 5.25 nm. Water atoms contact closely with workpiece and tool, even in the small gaps between the machined surface and the flank face of diamond tool. Newton layer of workpiece has divided into small grids in order to observe lattice deformation easily, it can be found that the crystalline structure near the shear zone is compressed, destroyed and amorphized as the tool moves forward. The atoms in the right side of workpiece also affected and twisted slightly during cutting, this possibly due to the number of atoms in the simulation cell are relatively small. The general contour appearance of chips in the two simulations, one with and the other without water atoms, seem resemble. However, a close examination of them shows that the chip size in vacuum simulation model is 8% larger than in water. The surface contour of chip in vacuum is shown as the blue line in Figure 2. One can find that the chip length is 0.12 nm longer in vacuum than in the fluid containing model. The temperature of water is much lower than chip which retarded the elastic recovery and activity of chip atoms. Additionally, the closely contacted water molecules with high temperature of chip atoms will be boiled away and resulted in a local higher pressure around the chip surface, the diffuse of chip atoms were limited.

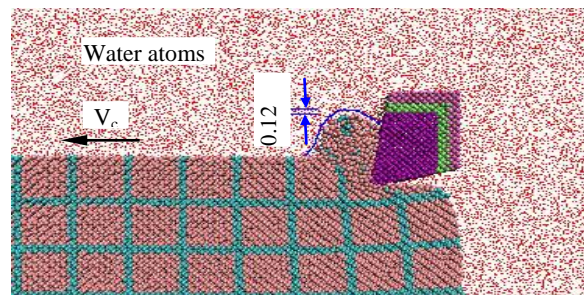


**Figure 2. The Cross-sectional Views of the Cutting process in the Fluid Containing Model**

#### 3.2 Heat Distribution

The temperature of fluid is controlled at 300 K after adding into the simulation model and acted as coolant. Furthermore, fluid provides a way to achieve heat equilibrium during machining. Figure 3 (a) and Figure 3 (b) show the heat distribution between with and without water, respectively. The various temperature ranges are coded by different colors to distinguish the temperature ranges of system during machining. In both cases, it can be found that the heat distribution topology is unanimous and roughly presents a concentric shape, a steep temperature gradient can be observed in tool and the highest temperature lies in chip.

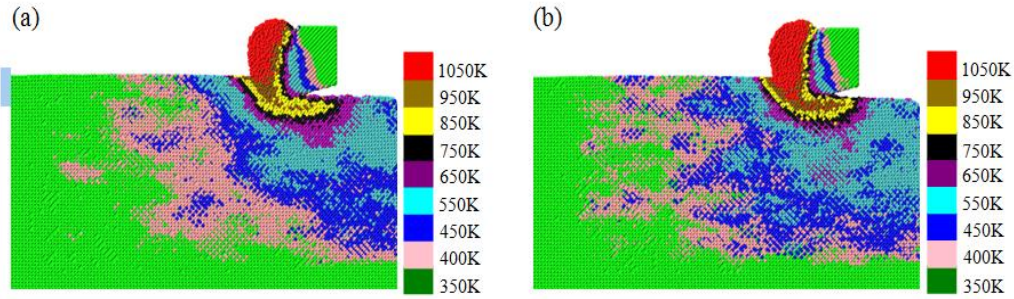


**Figure 3. The Cross-sectional Views of Heat Distribution at Cutting Distance of 10.5 nm**

When machining at vacuum condition (Figure 3 (b)), most of heat is taken away by chips, but the relative small chip size and lack of energy conversion raised the system temperature ultimately. The thermostat atoms (next to fixed layer) are so far away that they can not affect the temperature of Newton atoms significantly. Furthermore, the thermal conductivity of nanoscale silicon particles decrease significantly as the temperature increases, this decrease is thought to be the result of a reduced phonon mean free path (MFP) at elevated temperatures [13]. After adding water into the simulation cell, more heat can be “absorbed” by fluid. Figure 4 shows a comparison of the number of atoms in different temperature ranges between with and without water, and the corresponding cutting distance is 5.25 nm. After proportional convection is made, it can be found that the average temperature is decreased of 6% in the low temperature ranges and 15% in chips of the fluid containing model. A significant phenomenon is that there are about two layers atoms in the surface of tool rake face, which has a much lower temperature than in chips, the temperature of some tool atoms even lower than 350 K. Compared with silicon, diamond has a much higher heat conductivity and could transform heat faster, which result in a steep temperature gradient is appeared in diamond tool. Additionally, the temperature gradient is much distinctness in the fluid containing model.

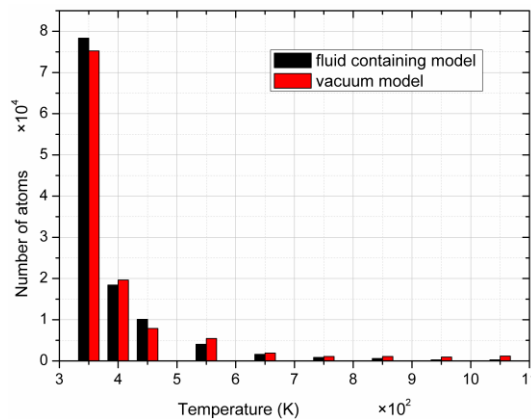


**Figure 4. The Number of Atoms in Different Temperature Ranges between with and without Water**

The high temperature region in shear zone means a buildup of large stress in a local region. Most of heat is generated by friction and excursion between tool and workpiece atoms, the atoms in shear zone with high temperature moves along the rake face of tool forward, bonds are broken and bond energy released due to the plastic deformation in workpiece material, almost all the chemistry and kinetic

energy are transformed into heat energy, the system temperature raised gradually with the increase of cutting length. In nanoscale, the flow stress of material is reduced due to rising of temperature, which indicates the decrease of workpiece material strength. The atoms vibrated more frequently and the distance between neighbor atoms increased with the raise of temperature, which inevitable result in weakening the bonding force between atoms. Surface and inner atoms have more energy at a high temperature and move easily when external force are imposed on the tool, that is why workpiece could be deformed under a relative low cutting force as the temperature rising. Large numbers of grain boundary provide a short cut for heat energy to diffuse from the shear zone to the inner of workpiece and promote the deformation of workpiece material.

### 3.3 Phase Transformations

In the past few years, extensive experiment works have been down to study phase transition of mono-crystalline silicon during machining [14, 15]. Experiment results show that twelve different structures and structure phase transformations have occurred. It has been generally accepted that the first phase transformation occurred from diamond cubic structure (Si-I) to the  $\beta$ -Si (Si-II), this was a nonmetal/metal transition. At higher pressure, five further high-pressure phases (Si-XI, Si-V, Si-VI, Si-VII, Si-X) were identified [16]. The structure phase transformation is studied through the technique of coordination number in workpiece. The coordination number of Si-I, Si-II and bct5-Si are fourfold, sixfold and fivefold coordinated, respectively. Figure 5 shows the cross-section views of the transformed region of the fluid containing model when the cutting distance is 12 nm. The coordination numbers in workpiece are marked by different colors. Aiming to analyze in greater detail of the amorphized atoms during machining, such atoms were isolated from the model. One can found that phase transition mainly occurred in the machined surface, shear zone and chips. The coordination numbers of atoms are mainly fivefold and sixfold in the machined surface and the coordination numbers of atoms more than tenfold are found in chips, which indicates that atoms in the machined surface were transformed from diamond cubic structure (Si-I) to the  $\beta$ -Si (Si-II) and bct5-Si. The amorphous phase was a mixture of atoms with coordination number equal to 4, 5 and 6 in the machined surface.

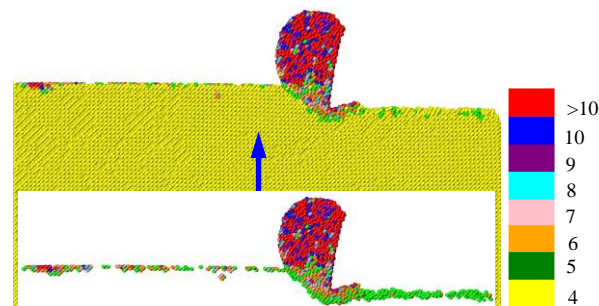


**Figure 5. The Cross-sectional Views of the Transformed Region of Work Piece in the Fluid Containing Model**

During machining with water, the volume of transformed silicon is found to be decreased 9% as shown in Figure 6. It seems that more atoms in the machined surface and chips transferred into amorphous silicon in the vacuum model. Atoms with coordination number of 7, 8 and 9 are not stable during machining and worked as metastable phase, these atoms mainly located in the shear zone. The friction and excursion between workpiece and tool build up large stress in a local region which breaks bond connection, the chemistry and kinetic energy are transformed into heat energy and rise the system temperature ultimately, after adding fluid into simulation model, more heat energy can be

“absorbed” by the cooling fluid, both the number of phase transfer atoms with the coordination numbers of five and six in the machined surface and the coordination number above ten in chips are much lower than machining in vacuum. However, in the shear zone (coordination number of 7, 8 and 9), few water atoms can diffused in it and the temperature disparity is indistinctness, the number of atoms with coordination number 7, 8 and 9 in both cases, as shown in Figure 6, were similarly.

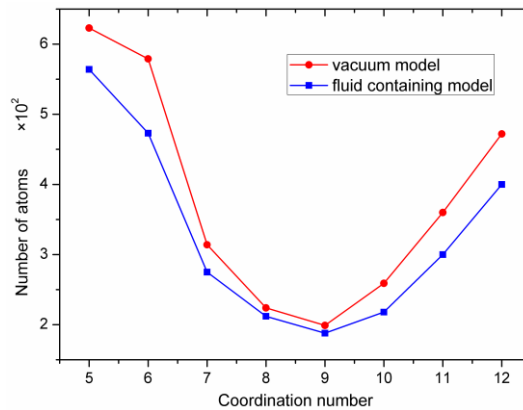


**Figure 6. Structure Changes of Work Piece during Machining between with and without Water**

#### 4. Conclusion

In the present work, the effects of fluid on the thermal behavior during nanometric cutting process were investigated from an atomic point of view. Earlier atomic simulations were focused on material removing mechanism and carried out in vacuum without considering the effect of external environment. Molecular dynamics method used in this work enabled in atomic scale analysis of chips formation, heat distribution and phase transformation after taking fluid into account.

The present simulations have revealed the following insights:

- (1) Taking fluid into account represents a more completely thermal equilibrium and heat convection during machining.
- (2) The chip size is 8% larger in vacuum than in the fluid containing model at the same simulation stage.
- (3) In contrast to the situation of nanometric cutting in vacuum, the average temperature is decreased of 6% in the low temperature ranges and 15% in chips of the fluid containing model. In both case, however, the heat distribution topology is unanimous and roughly presents a concentric shape, a steep temperature gradient can be observed in tool and the highest temperature lies in chip.
- (4) The phase transformation mainly occurred in the machined surface, shear zone and chips. After adding fluid into simulation, the growth of phase transformation is retarded 9%.

It is clear that although the chip generation, heat distribution and phase transformation in the two case is similar, the magnitude and size of chip length, high temperature and coordination number are different, furthermore, considering the size of the simulation cell and simulated process time, the impact of fluid on nanometric cutting process must be rated as high. Future work is needed to study the chemical role of water, inclusion of tool wear, adsorption or reaction of fluid during machining would be a logical continuation of this work.



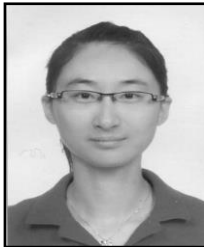
## Acknowledgements

The authors gratefully acknowledge both the China Postdoctoral Science Foundation (No.2013M530152) and the Fundamental Research Funds for Central Universities (No.HIT.NSRIF.2015055) for their financial supports of this work.

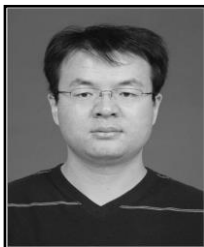
## References

- [1] M. D. Segall, P. J. D. Lindan, M. J. Probert, *et al.*, J. Phys.: Condens. Matter, vol. 14, no. 2717, (2002).
- [2] U. Heisel, M. Storchak and D. Krivoruchko, Prod. Eng. Res. Devel, vol. 7, no. 203, (2013).
- [3] Y. Ye, R. Biswas, J. R. Morris, A. Bastawros and A. Chandra, Nanotechnology, vol. 14, no. 390, (2003).
- [4] M. Lai, X. D. Zhang, F. Z. Fang, *et al.*, Nanoscale Res. Lett., vol. 8, no. 13, (2013).
- [5] Y. B. Guo, Y. C. Liang, M. J. Chen, *et al.*, Sci. China Tech. Sci., vol. 53, no. 870, (2010).
- [6] J. X. Chen, Q. L. Wang, Y. C. Liang, *et al.*, Procedia Eng., vol. 29, no. 3478, (2012).
- [7] R. Rentsch and I. Inasaki, Ann. CIRP., vol. 55, no. 601, (2006).
- [8] Y. Lin and T. Inamura, JSME, vol. 49, no. 70, (2006).
- [9] J. Tersoff, Phys. Rev. B., vol. 39, no. 5566, (1989).
- [10] M. B. Cai, X. P. Li and M. Rahman, J. Manuf. Sci. Eng., vol. 129, no. 281, (2007).
- [11] F. Z. Fang, H. Wu, W. Zhou and X. T. Hu, J. Mater. Process. Technol., vol. 184, no. 407, (2007).
- [12] L. W. Li, D. Bedrov and G. D. Smith, Phys. Rev. E., vol. 71, no. 011502, (2005).
- [13] K. C. Fang, and C. I. Weng, Nanotechnology, vol. 17, no. 3909, (2006).
- [14] J. Crain, S. J. Clark and G. J. Ackland, Phys. Rev. B., vol. 49, no. 5329, (1994).
- [15] J. Crain, G. J. Ackland and J. R. Maclean, Phys. Rev. B., vol. 50, no. 13043, (1994).
- [16] J. Z. Hu, L. D. Merkle and C. S. Menoni, Phys. Rev. B., vol. 34, no. 4679, (1986).

## Authors



**Guokun Qu** received her B.S. degree in Basic Mathematics from Harbin University of Science and Technology in 2007. She is working as Lecturer in Harbin University of Commerce. Her research interest fields are differential equations and complex system.



**Yongbo Guo** received his PhD degree in Mechanical Engineering from Harbin Institute of Technology in 2011. He is working as Lecturer in Center for Precision Engineering. His research interest fields are ultra-precision processing technology and nanotechnology.

